DOI: https://doi.org/10.15407/pmach2021.03.045

UDC 539.3

ANALYSIS OF STRESS-STRAIN STATE AND CONTACT PRESSURES ON SURFACES OF KAPLAN RUNNER BLADE BEARING BRONZE BUSHES

[1] Viktor H. Subotin, office@turboatom.com.ua
ORCID: 0000-0002-2489-5836

[1] Oleksandr S. Burakov, burakov.a.b.s@gmail.com
ORCID: 0000-0002-3264-5300

[1] Oleksii V. Dushyn
ORCID: 0000-0002-1549-5152

[1] Viktor M. Iefymenko, efimenko@turboatom.com.ua
ORCID: 0000-0003-2140-893X

[1] Oleksii O. Korshunov,
korshunov_ao@turboatom.com.ua
ORCID: 0000-0002-3386-5372

[2] Oleg M. Khoryev, oleg_xo@ukr.net
ORCID: 0000-0001-6940-4183

[1] JSC "Turboatom"
199, Moskovskyi ave., Kharkiv, 61037, Ukraine

[2] A. Pidhornyi Institute of Mechanical Engineering Problems of NASU
2/10, Pozharskyi str., Kharkiv, 61046, Ukraine

An analysis of the existing and prospective blade seal designs for Kaplan runners was performed. The selected design type provides the maximum ecological safety for Kaplan runners. A 3D model of runner hub sector with the trunnion, inner and outer bushes of blade trunnion was generated taking into account the cyclic symmetry of the runner design based on the modern automated design engineering system. A diagram of application of external loads from the blade and lever to the given 3D model of the Kaplan runner hub segment was developed. The contact problem was formulated to determine the stress-strain state as well as the contact pressures at the inner and outer bronze bushes of the Kaplan runner blade trunnions in different operating conditions. The problem was formulated for the finite element method, taking into consideration the diagram of external load application and contact restraints to the given 3D model of the Kaplan runner hub sector in the software package for engineering calculations. Using calculation results, principal stress distribution diagrams and the distribution diagram for the contact pressure at the outer and inner bronze bushes of blade trunnions were obtained. Strength calculation results were processed using the data of principal stress distribution diagrams, and the contact pressure values at the inner and outer bronze bushes of blade trunnions were determined. A methodology for further use of the given analytical model in the evaluation of stress-strain state of Kaplan runners involving modern automated design engineering systems and software package for engineering calculations was developed. The comparison of stress-strain states of the blade trunnion bushes was performed for the old and new designs of the Kaplan runner seal.

Keywords: *bearing bushes; runner; finite element method; contact problem; mathematical model.*

Introduction

The experience of JSC "Turboatom" in runner modernization for horizontal bulb hydro-units shows that the new blade trunnion bronze bushes within the bearing group in the runner holes have a complex stress-strain state while the old blade trunnion bushes used to be subject to compressive loads mainly. During runner modernization involving the design of the existing seal [1], it becomes necessary to apply a new design of blade trunnion bronze bushes, with a prominent cantilever portion to accommodate the newly-designed seal. This results in a considerable redistribution of the stress-strain state as compared to that of the initial seal type. Thus, in order to guarantee the bearing assembly operability, one shall take into consideration the complete range of loads transferred to the bush from the *blade / trunnion / lever* system.

Analytical model description

The cyclic symmetry of the structure allows to analyse the stress-strain state of its mathematical model by means of modelling of a typical segment [2], which can be a part or an assembly. The segment shape, displacement restraints, and working loads shall be similar for all the cycling segments forming the structure. Taking into consideration the cyclic symmetry of the structure, in order to determine the stress-strain state and

contact pressures on the surfaces of the blade trunnion bronze bushes within the runner blade bearing assembly, a contact problem for an assembly comprising a segment of the runner hub (1/4 runner hub), trunnion, inner and outer bronze bushes of the blade trunnions is solved. Contact interaction on the friction surfaces between the blade trunnion bronze bushes and blade trunnion as well as on the surfaces of blade trunnion bronze bushes in the areas of bush pressing into the runner hub is specified. Figure 1 shows the analytical model.

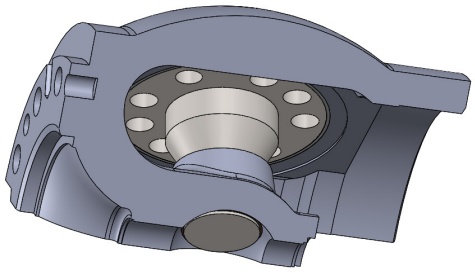

Fig. 1. Model for assembly analysis

Figure 2 shows a mathematical model section by *OZ* plane going through the blade trunnion axis of rotation as well as through the turbine axis. The restrained surfaces are indicated in the section as well as surfaces on which the contact conditions are specified for the parts included in the assembly described below.

The mathematical model is discretized by a TETRA10 parabolic tetrahedral solid element being a tetrahedron with curved faces which has nodes at its vertices and side midpoints. The nodes of the finite element have three degrees of freedom (ref. to Fig. 3). Figure 4 shows the finite element model, loads, and conditions.

To solve the problem in contact formulation [3] the following types of contact between the structure elements are specified:

– on the friction surfaces between the blade trunnion bronze bushes and blade trunnion: *No Penetration*. Such contact type excludes any interference between the contact objects while still allowing a gap between the above objects;

– on the surfaces of bronze bushes of blade trunnion, in the areas of bush pressing-in: *Bonded*. Such contact type binds each node of the finite element on the contact surface of the first target object i.e., the bush to the nearest face of other target object i.e., runner hub rigidly (not allowing any gap or interference).

The cyclic symmetry conditions are set on the cut off faces of the runner hub segment.

In the bolt holes of the runner hub segment, another restraint type is set i.e., *Fixed*. Such a restraint type restrains three translational degrees of freedom for a solid body.

The trunnion on the lever seating surface is restrained by *No rotation on cylindrical face* restraint type. This assumption is introduced into the mathematical model to prevent stress concentration at the location points of the keys transferring torque from the lever to the blade.

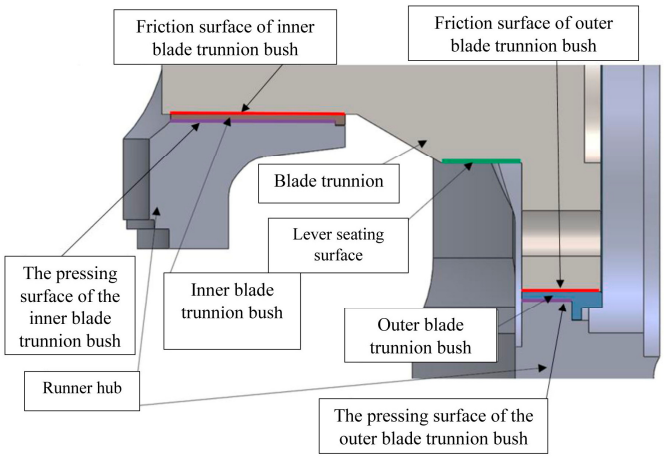

Fig. 2. Analytical model section by plane OZ

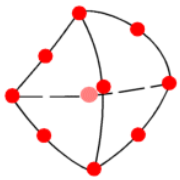

Fig. 3. Physical configuration of TETRA10 finite element

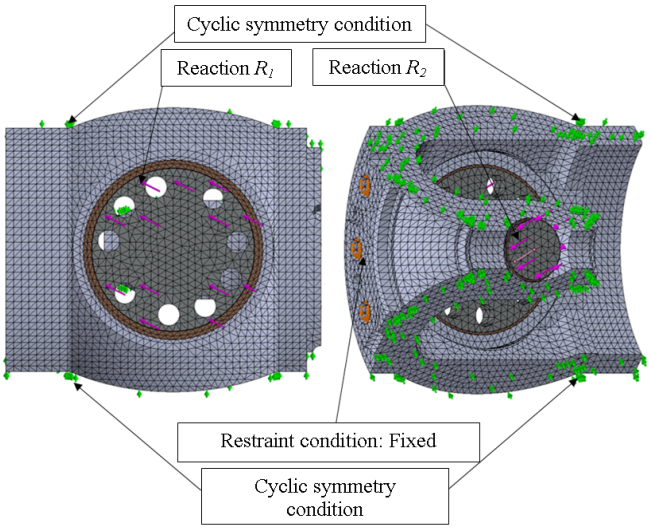

Fig. 4. Finite element model for assembly analysis

The acting loads are the reaction at the inner R_1 and outer R_2 supports of the trunnion. The load values, values of load projections R_X and R_Y on the coordinate axes are determined in the calculation of servomotor required forces. In this calculation, the coordinate axes are local for the finite element model of the assembly. Loads are applied to the blade trunnion end-faces in the finite element model, with this contributing to the safety margin. Figure 4 shows the load application points in the finite element model of the assembly as well as the action direction.

The stress-strain state of the blade trunnion bronze bushes is determined for the turbine operating conditions in which reactions either at the inner or at the outer trunnion support are maximum. Table 1 shows reaction R_1 and R_2 values as well as runner servomotor operating modes description.

The orientation of reactions (Table 1) relative to the *Y*-axis of the global coordinates is determined taking into consideration the reaction projections R_X and R_Y on the coordinate axes which are calculated in the calculation of the required servomotor force. Table 2 and Figure 5 show the values and directions of the reactions R_1 and R_2, reaction projections R_{Xi} and R_{Yi}, and angles α and β defining the orientation of R_1 and R_2 in the *XY* plane within the system of global coordinates *X, Y, Z*.

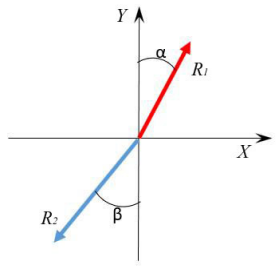

Fig. 5. Orientation of resultants within global coordinate system

Table 1. Operating conditions with maximum reactions at inner and outer trunnion support

Operating mode	Operating conditions	R_1, kN	R_2, kN	Note
Mode 1	Required servomotor force during piston closing stroke	1907	2640	R_{2max}
Mode 2	Required servomotor force during piston opening stroke	3193	2549	R_{1max}
Mode 3	Maximum servomotor force during piston closing stroke	982	2731	R_{2max}
Mode 4	Maximum servomotor force during piston opening stroke	3552	2232	R_{1max}

Table 2. Reaction orientation within global coordinate system

Operating mode	R_X, kN	R_Y, kN	R_1, kN	α, °	Rx, kN	R_Y, kN	R_2, kN	β, °
Mode 1	901	1681	1907	28.195	1177	2363	2340	26.483
Mode 2	863	3074	3193	15.687	1180	2259	2549	27.576
Mode 3	938	291	982	72.798	1174	2466	2732	25.465
Mode 4	853	3448	3552	13.900	1181	2232	2525	27.883

Calculation results

At each contact point of adjoining parts and parts included into the assembly, three-dimensional (triaxial) stress state occurs, which is illustrated by the distribution diagrams of the principal stresses σ_1, σ_2, σ_3, for Mode 1 (Figs. 6–11). Thus, Figs. 6–8 show distribution of the principal stresses in the OR_2 plane going through the trunnion rotation axis as well as reaction R_2 at the outer trunnion support while Figs. 9–11 show distribution of the principal stresses in the OR_1 plane going through the trunnion rotation axis as well as reaction R_1 at the inner trunnion support.

Taking into consideration the low ductility of bronze "Br.O10F1" (its unit elongation being equivalent to $\delta_5 \geq 3\%$ [4]), for the purpose of bush strength determination, we use the criterion of the largest linear deformations as per which for materials that are subject to Hooke's law, a failure or start of plastic deformation occurs when the linear deformation having the largest absolute value reaches a definite boundary value [5, 6].

According to the above criterion, for an equivalent stress state i.e., uniaxial tension, the equivalents stresses σ_{equiv} are determined from the following expression:

$$\sigma_{equiv} = \sigma_1 - \mu(\sigma_2 + \sigma_3),$$

where $\sigma_1, \sigma_2, \sigma_3$ are the principal stresses; μ is the Poisson's ratio for bronzes, lying within μ=0.32…0.35.

In further calculations, μ=0.35 is adopted, this contributing to the safety margin of the structure.

The maximum allowable stresses during a check for the maximum static or peak load are determined as follows [7]:

$$[\sigma] = 0{,}8\sigma_y = 0{,}8 \cdot 140 = 112 \text{ MPa},$$

where σ_y is the yield point of bronze "Br.O10F1".

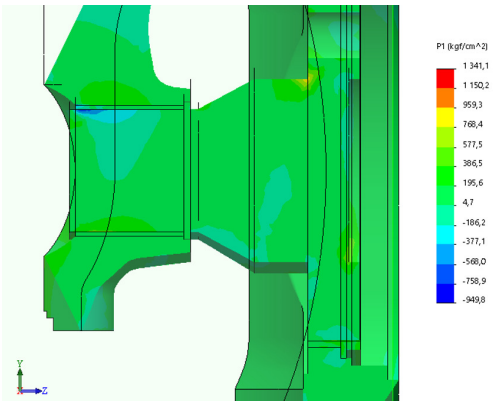

Fig. 6. Distribution of principal stresses σ_1 in OR_2 plane in turbine operating mode

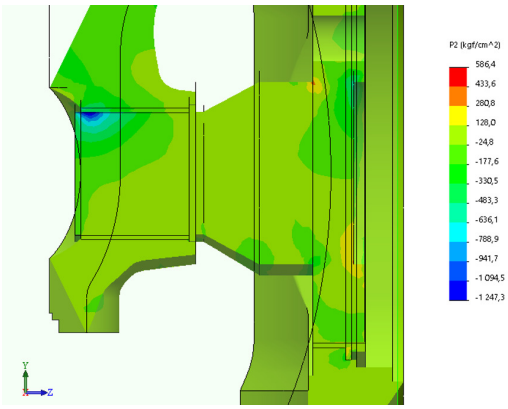

Fig. 7. Distribution of principal stresses σ_2 in OR_2 plane in turbine operating mode

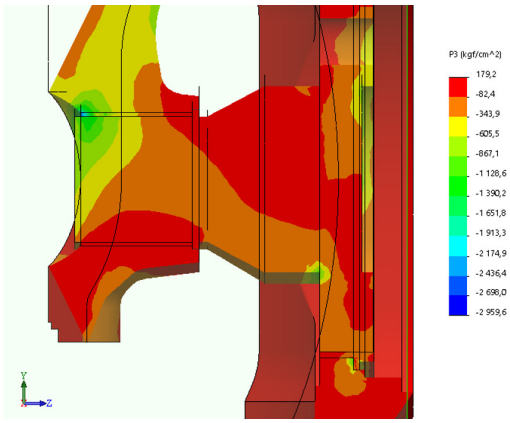

Fig. 8. Distribution of principal stresses σ_3 in OR_2 plane in turbine operating mode

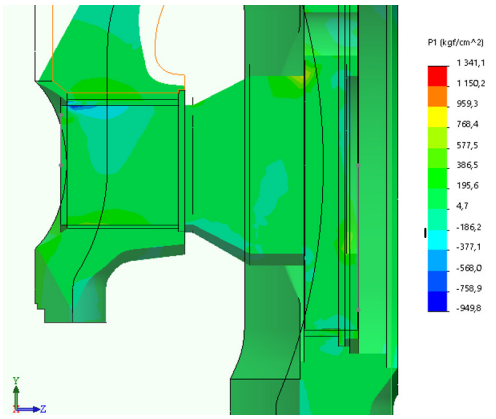

Fig. 9. Distribution of principal stresses σ_1 in OR_1 plane in turbine operating mode

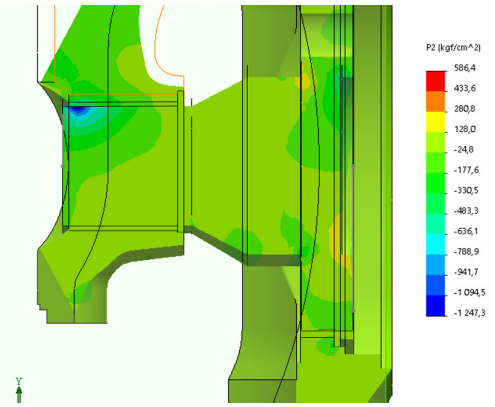

Fig. 10. Distribution of principal stresses σ_2 in OR_1 plane in turbine operating mode

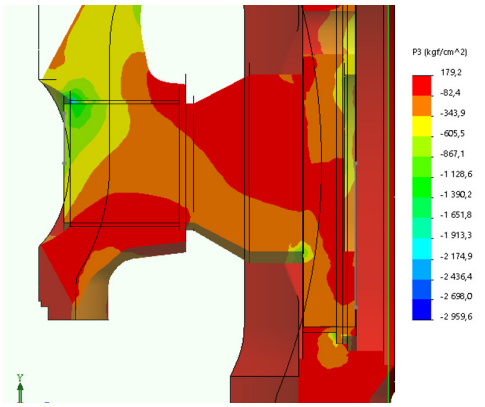

Fig. 11. Distribution of principal stresses σ_3 in OR_1 plane in turbine operating mode

It is more reasonable to determine the stress-strain state of the outer blade trunnion bushes by the values of the principal stresses at the characteristic points *A* and *B*. Figure 12 shows the arrangement of the above points while Table 3 lists the values of the principal stresses σ_1, σ_2, σ_3 and equivalent stresses σ_{equiv}. In a similar manner, the stress-strain state of the inner blade trunnion bushes can be described taking as a basis the values of the above stated principal and equivalent stresses at the points *C* and *D,* which arrangement is shown in Figure 13 and which values are shown in Table 4.

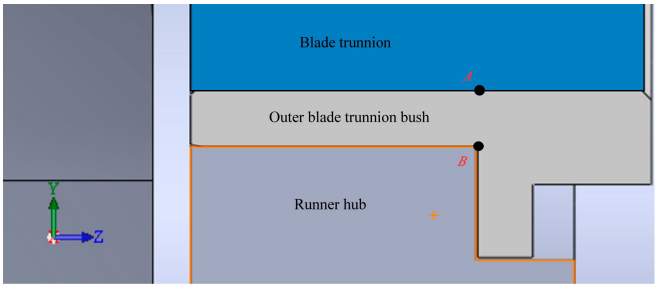

Fig. 12. Arrangement of characteristic points **A** *and* **B** *to determine stress-strain state of outer blade trunnion bush*

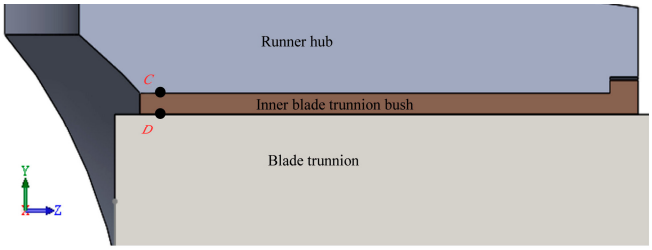

Fig. 13. Arrangement of characteristic points **C** *and* **D** *to determine stress-strain state of inner blade trunnion bush*

Table 3. Values of principal and equivalent stresses at outer runner bush

Operating mode	Stress component	Working stress value, MPa	
		Hub side, point *A*	Load side, point *B*
Mode 1	σ_1	22.5	32.4
	σ_2	11.8	11.8
	σ_3	–7.8	–22.1
	σ_{equiv}	21.2	36.0
Mode 2	σ_1	23.5	44.1
	σ_2	16.7	12.8
	σ_3	–8.8	–26.5
	σ_{equiv}	20.8	49.0
Mode 3	σ_1	19.6	37.3
	σ_2	10.3	13.7
	σ_3	–6.9	–19.6
	σ_{equiv}	18.4	39.3
Mode 4	σ_1	19.1	34.8
	σ_2	11.3	11.3
	σ_3	–10.8	–22.1

Table 4. Values of principal and equivalent stresses at inner blade trunnion bush

Operating mode	Stress component	Working stress value, MPa	
		Hub side, point *C*	Load side, point *D*
Mode 1	σ_1	–60.8	–11.9
	σ_2	–69.2	–38.7
	σ_3	–258.0	–234.5
	σ_{equiv}	53.7	83.8
Mode 2	σ_1	–90.3	–54.0
	σ_2	–102.0	–67.2
	σ_3	–392.4	–392.4
	σ_{equiv}	82.8	106.9
Mode 3	σ_1	–23.5	–11.8
	σ_2	–32.4	–28.4
	σ_3	–111.3	–99.1
	σ_{equiv}	26.8	32.9
Mode 4	σ_1	–100.1	–55.9
	σ_2	–112.8	–82.4
	σ_3	–418.9	–384.6

A similar analysis of the structure stress-strain state in the area of the outer blade trunnion bushes with the old seal in operation was performed for a comparison. Table 5 lists values of the principal and equivalent stresses at the *E* and *F* points and Figure 14 shows the point arrangement. The inner blade trunnion bushes within the bearing group are not re-engineered so one can believe that the stress-strain state pattern will be similar for the old and new runner seal types.

Fig. 14. Arrangement of characteristic points E and F to determine stress-strain state of outer blade trunnion bush with old seal design

Table 5. Values of principal and equivalent stresses at outer blade trunnion bush with old seal design

Operating mode	Stress component	Working stress value, МПа	
		Hub side, point *E*	Load side, point *F*
Mode 1	σ_1	–30.4	29.4
	σ_2	–36.3	–58.9
	σ_3	–29.4	–57.9
	σ_{equiv}	–7.5	70.3
Mode 2	σ_1	–33.0	39.7
	σ_2	–50.6	–63.0
	σ_3	–35.5	–70.1
	σ_{equiv}	–2.8	86.3
Mode 3	σ_1	–26.5	33.8
	σ_2	–33.0	–70.6
	σ_3	–27.3	–49.3
	σ_{equiv}	–5.4	74.9
Mode 4	σ_1	–25.8	31.7
	σ_2	–34.8	–56.4
	σ_3	–40.5	–57.9
	σ_{equiv}	0.6	71.6

Besides the blade trunnion bush strength, the values of contact pressures acting on the bearing bush working surfaces are also an operability criterion for the bushes. Solving of the problem in three-dimensional formulation allows full evaluation of the contact pressure distribution diagram and operability of the modernized runner blade seal. Figure 15 shows the diagram of contact pressure distribution on the working surface of the outer blade trunnion bush within the bearing group while Table 6 lists values of the maximum operating and maximum allowable contact pressures.

Table 6. Values of maximum operating and maximum allowable contact pressures at outer blade trunnion bush

Mode of operation	Maximum operating contact pressure, MPa	Maximum allowable contact pressure, MPa
Mode 1	30.1	44.1
Mode 2	28.9	
Mode 3	28.0	63.8
Mode 4	32.4	

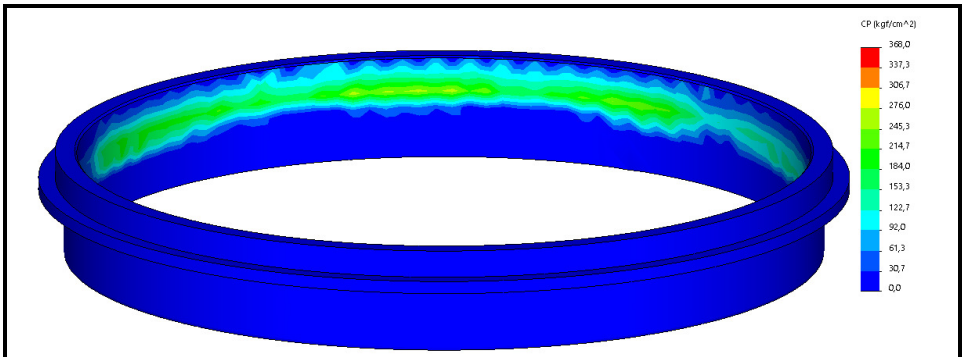

Fig. 15. Contact pressure distribution diagram for Ø850 mm bush, Mode 1

Conclusions

As can be seen from the above, a thorough analysis of the stress-strain state of the modernized blade trunnion bushes within the bearing group suggests that the new blade trunnion bush design provides the reliability required to accommodate the modernized seal and allows manufacturing of new runners which not only meet the strict strength and design production-friendliness requirements but also provide high ecological safety of such runners.

References

1. Kovalev, N. N. (1971). *Gidroturbiny. Konstruktsii i voprosy proyektirovaniya* [Hydroturbines. Constructions and design issues.]. Leningrad: Mashinostroyeniye, 584 p. (in Russian).
2. Guznekov, V. N., Zhurbenko, P. A., & Borodayeva, T. P. (2017). *Solidworks 2016: Trekhmernoye modelirovaniye i vypolneniye elektronnykh chertezhey* [Solidworks 2016: Three-dimensional modeling and execution of electronic drawings]. Moscow: N. E. Bauman Moscow Technical University Publ., 124 p. (in Russian).
3. Alyamovskiy, A. A., Sobachkin, A. A., Odintsov, Ye. V., Kharitonovich, A. I., & Ponomarev, N. B. (2005). *Kompyuternoye modelirovaniye v inzhenernoy praktike* [Computer modeling in engineering practice]. St. Petersburg: BKhV-Peterburg, 783 p. (in Russian).
4. (2000). *GOST 613-79. Bronzy olovyannyye liteynyye. Marki.* [Foundry tin bronzes. Stamps.]: Introduced January 01 1980. Moscow: 5 p. (in Russian).
5. Goldenblat, I. I. & Kopnov, V. A. (1968). *Kriterii prochnosti i plastichnosti konstruktsionnykh materialov* [Criteria of strength and plasticity of structural materials]. Moscow: Mashinostroyeniye, 191 p. (in Russian).
6. Ponomarev, S. D., Biderman, V. L., & Sosnovskiy, L. A. (1956). *Raschety na prochnost v mashinostroyenii Soprotivleniye ustalosti metallov i splavov* [Strength calculations in mechanical engineering. Fatigue resistance of metals and alloys]: Handbook in 2 parts. Moscow: Mashgiz, 191 p. (in Russian).
7. Vasilkov, D. B., Veyts, V. L., & Skhirtladze, A. G. (2010). *Elektromekhanicheskiye privody metalloobrabatyvayushchikh stankov. Raschet i konstruirovaniye* [Electromechanical drives of metalworking machines. Calculation and design]. St. Petersburg: Politekhnika, 759 p. (in Russian).

Received 29 July 2021

Аналіз напружено-деформованого стану та контактних тисків на поверхнях бронзових втулок підшипника лопаті поворотно-лопатевого робочого колеса

[1] В. Г. Суботін, [1] О. С. Бураков, [1] О. В. Душин, [1] В. М. Єфименко, [1] О. О. Коршунов, [2] О. М. Хорєв

[1] АТ «Турбоатом», 61037, Україна, м. Харків, пр. Московський, 199

[2] Інститут проблем машинобудування ім. А. М. Підгорного НАН України, 61046, Україна, м. Харків, вул. Пожарського, 2/10

Виконано аналіз існуючих та перспективних конструкцій ущільнення лопатей для робочих коліс поворотно-лопатевого типу. Обраний тип ущільнення забезпечує максимальну екологічність для робочих коліс поворотно-лопатевого типу. Побудовано тривимірну модель сектора корпусу робочого колеса із встановленою цапфою та внутрішньою і зовнішньою втулками цапфи лопаті з урахуванням циклічної симетрії конструкції робочого колеса на базі сучасної системи автоматичного проектування. Розроблено схему прикладання зовнішніх навантажень від лопаті та важеля на наведену тривимірну модель сектора корпусу робочого колеса поворотно-лопатевого типу. Здійснено постановку контактної задачі для визначення напружено-деформованого стану та контактних тисків внутрішньої та зовнішньої бронзових втулок цапфи лопаті поворотно-лопатевого робочого колеса за різних режимів роботи. Виконано постановку задачі для методу скінченних елементів із урахуванням схеми прикладання зовнішніх навантажень та контактних обмежень на наведену тривимірну модель сектора корпусу робочого колеса поворотно-лопатевого типу у програмному комплексі для виконання інженерних розрахунків. За результатами розрахунків отримано епюри розподілу головних напружень та епюру розподілу контактного тиску на зовнішній та внутрішній бронзових втулках цапфи лопаті. Опрацьовано результати розрахунків на міцність за даними епюр розподілу головних напружень та визначено контактний тиск на внутрішній та зовнішній бронзових втулках цапфи лопаті. Розроблено методику для подальшого використання наведеної розрахункової схеми при оцінці напружено-деформованого стану деталей робочих коліс поворотно-лопатевого типу з використанням сучасних систем автоматичного проектування та програмного комплексу для виконання інженерних розрахунків. Виконано порівняння напружено-деформованого стану втулок цапфи лопаті для старої та нової конструкції ущільнення робочого колеса поворотно-лопатевого типу.

***Ключові слова**: втулки підшипників, робоче колесо, метод скінченних елементів, контактна задача, математична модель.*

Література

1. Ковалев Н. Н. Гидротурбины. Конструкции и вопросы проектирования. Л.: Машиностроение, 1971. 584 с.
2. Гузнеков В. Н., Журбенко П. А., Бородаева Т. П. Solidworks 2016: Трехмерное моделирование и выполнение электронных чертежей. М.: Изд-во Моск. техн. ун-та им. Н. Э. Баумана, 2017. 124 с.
3. Алямовский А. А., Собачкин А. А., Одинцов Е. В., Харитонович А. И., . Пономарев Н. Б. Компьютерное моделирование в инженерной практике. СПб.: БХВ-Петербург, 2005. 783с.
4. ГОСТ 613-79. Бронзы оловянные литейные. Марки. Введ. 1980-01-01. М., 2000. 5 с.
5. Гольденблат И. И., Копнов В. А. Критерии прочности и пластичности конструкционных материалов. М.: Машиностроение, 1968. 191 с.
6. Пономарев С. Д., Бидерман В. Л., Сосновский Л. А. Расчеты на прочность в машиностроении. Сопротивление усталости металлов и сплавов. Справочник: в 2–х ч. М.: Машгиз, 1956. 191 с.
7. Васильков Д. Б., Вейц В. Л. , Схиртладзе А. Г. Электромеханические приводы металлообрабатывающих станков. Расчет и конструирование. СПб.: Политехника, 2010. 759 с.